SEECCM III
3rd South-East European Conference on Computational Mechanics
An ECCOMAS and IACM Special Interest Conference
M. Papadrakakis, M. Kojic, I. Tuncer (eds.)
Kos Island, Greece, 12–14 June 2013

MODELING THE FAILURE OF STRUCTURES WITH STOCHASTIC PROPERTIES IN A SEQUENTIALLY LINEAR ANALYSIS FRAMEWORK

Manolis Georgioudakis[1*], George Stefanou[1,2] and Manolis Papadrakakis[1]

[1]Institute of Structural Analysis & Antiseismic Research
School of Civil Engineering
National Technical University of Athens
Zografou Campus, 15780 Athens, Greece

[2] Institute of Structural Analysis & Dynamics of Structures
Department of Civil Engineering
Aristotle University of Thessaloniki
54124 Thessaloniki, Greece
e-mail: {geoem,stegesa}@mail.ntua.gr, mpapadra@central.ntua.gr

Keywords: sequentially linear analysis, saw-tooth softening, stochastic finite element, Monte Carlo simulation

Abstract. *This paper investigates the influence of uncertain spatially varying material properties on the fracture behavior of structures made of softening materials. To model the structural failure, the sequentially linear solution procedure proposed by Rots (2001) is used, which replaces the incremental (nonlinear) finite element analysis by a series of scaled linear analyses and the nonlinear stress-strain law by a saw-tooth curve. The effect of uncertain material properties (Young's modulus, tensile strength, fracture energy) on the variability of the load-displacement curves and crack paths is examined. The uncertain properties are described by homogeneous stochastic fields using the spectral representation method in conjunction with translation field theory. The response variability is computed by means of direct Monte Carlo simulation. The influence of the variation of each random parameter as well as of the probability distribution, coefficient of variation and correlation length of the stochastic fields is quantified. It is shown that the response statistics are affected by the spectral characteristics of the stochastic fields.*

1 INTRODUCTION

In recent years, several numerical techniques have been developed to model the failure of structures in the framework of the finite element method (FEM). There are two essential proposed approaches which are dealing with physical discontinuities (e.g. cracks, slip lines) by enriching the (continuous) displacement field of standard finite elements either on nodal level [5] (Extended Finite Element Method - XFEM) or on elemental level [6] (Embedded Finite Element Method - EFEM). Unlike with standard finite elements, mesh refinement is not necessary in these methods to capture the discontinuities and the simulation can be performed with relatively coarse meshes. A comparative study of the two approaches can be found in [7] but the detailed assessment of relative errors, rates of convergence and computational cost is still an open area of research.

It is well-known in failure mechanics that material softening is often responsible for unstable structural behavior [1]. Even if the boundary value problem is mathematically well posed, instabilities may arise in the incremental (nonlinear) solution schemes used in the aforementioned FE methods due to negative tangent stiffness. These instabilities can lead to more than one solution of the system of equations and thus to alternative equilibrium states or bifurcations of the equilibrium path. As a consequence, the robustness of the numerical procedure used for solving the nonlinear problem is strongly affected. In order to overcome these problems, an alternative method, called Sequentially Linear Analysis (SLA), has been introduced by Rots [9]. This method replaces the incremental (nonlinear) FE analysis by a series of scaled linear analyses and the nonlinear stress-strain law by a saw-tooth curve.

In this paper, SLA is implemented in a stochastic setting to investigate the influence of uncertain spatially varying material properties on the fracture behavior of structures made of softening materials. A benchmark structure (notched beam) is analyzed and comparisons with nonlinear analysis results are provided. The effect of uncertain Young's modulus, tensile strength and fracture energy on the variability of the load-displacement curves and crack paths is examined. The uncertain properties are described by homogeneous stochastic fields using the spectral representation method in conjunction with translation field theory [13], [4]. The response variability is computed by means of direct Monte Carlo simulation. The influence of the variation of each random parameter as well as of the probability distribution, coefficient of variation and correlation length of the stochastic fields is quantified. It is shown that the response statistics are affected by the spectral characteristics of the stochastic fields.

2 BRIEF REVIEW OF SEQUENTIALLY LINEAR ANALYSIS (SLA)

Modeling fracture through an *event-by-event* cracking procedure by imposing an increment of damage, is an attractive alternative to typical nonlinear FE analysis, where modeling proceeds by imposing increment of displacement or force. In this way, it is unnecessary to make large jumps in damage during a single load or displacement step, which is usually the source of convergence problems. To capture brittle events directly with SLA there is no need to iterate around these critical points.

To this purpose, a tensile softening curve of negative slope is replaced by a series of saw-teeth which maintain a positive tangent stiffness (see Fig. 1). The incremental/iterative Newton-Raphson method is replaced by a series of linear analyses, each with a reduced positive stiffness, until the global analysis is complete. It has been shown that this *event-by-event* strategy is robust and reliable [10], and circumvents bifurcation problems, in contrast to regular nonlinear FE analysis.

A brief review of SLA is provided below. More details about this method can be found in [2] and [3].

2.1 General procedure

The structure is discretized in the framework of standard FEM, using elastic continuum elements and all material properties (Young's modulus, Poisson's ratio and initial strength) are initially assigned to them. Subsequently, the following steps are carried out sequentially without need of changing the initial mesh:

- Perform a linear-elastic FE analysis with a unit external load and calculate the principal stresses;
- Loop over all integration points for all elements and find the *critical element* for which the stress level divided by its current strength is the highest in the whole structure;
- Calculate the critical load multiplier, belonging to the critical integration point, i.e. the current strength divided by the stress level;
- Scale the reference load proportionally by the critical load multiplier;
- Increase the damage in the critical integration point by reducing the stiffness E and strength f_t according to the saw-tooth tensile-based constitutive relation (see Section 2.2);
- Repeat the previous cycle of steps continuously, until the damage has spread sufficiently into the structure.

In this way, the nonlinear response is extracted by linking consecutively the results of each cycle. The smoothness of $P - \delta$ curves depends of course on the smoothness (number N of teeth) of the saw-tooth model (see Section 2.2). The SLA procedure allows only one integration point to change its status from elastic to softening at each time, while in nonlinear FE analysis, the use of load increments implies that multiple integration points may crack simultaneously and the local stiffnesses at these points switch from positive to negative, following the softening constitutive laws for quasi-brittle materials.

2.2 Saw-tooth model

In this work, the generalized tooth size approach (Model C) [11] with no requirement of special techniques to handle mesh-size objectivity is adopted, in order to obtain objective results with respect to the mesh as well as to overcome the lack of consistency. The way in which the stiffness and strength of the critical elements are progressively reduced at each ”event”, is shown schematically in Fig. 1 where the softening curve of negative slope in the constitutive stress-strain relation is replaced by a discretized saw-tooth diagram of positive slopes which provides the correct energy dissipation. The linear softening stress-strain curve is defined by the Young's modulus E, the tensile strength f_t and the area under the saw-tooth diagram. This area, (see Fig. 1) is always equal to the fracture energy G_f (which is considered here as a material property) divided by the crack bandwidth h, which is associated with the size, orientation and integration rule of the finite element. In case of linear softening, the ultimate strain ϵ_u is given by:

$$\epsilon_u = \frac{2G_f}{f_t h} \tag{1}$$

Both Young's modulus E and strength f_t can be reduced at the same time in the sequentially linear strategy by a factor a, according to:

$$E_i = \frac{E_{i-1}}{a}, \quad for \quad i = 1, 2, ..., N \tag{2}$$

where i and $i-1$ denote the current and previous step, respectively, in the saw-tooth diagram. To find the rule of reducing Young's modulus E as well as strength f_t by ratio a_i in step i according to Fig. 1, we have:

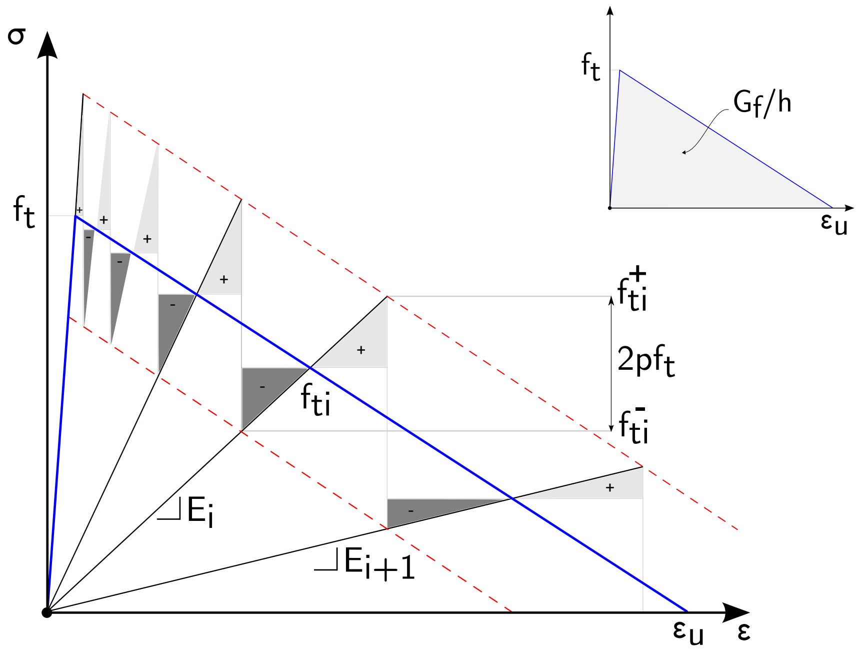

Figure 1: Saw-tooth model and definition of G_f

$$f_{ti}^{-} = f_{ti}^{+} - 2pf_t \tag{3}$$

$$E_{i+1} = \frac{f_{ti}^{-}}{\epsilon_i} \tag{4}$$

$$a_{i+1} = \frac{E_i}{f_{ti}^{-}}\epsilon_i = \frac{f_{ti}^{+}}{f_{ti}^{-}} = \frac{f_{ti}^{+}}{f_{ti}^{+} - 2pf_t} \tag{5}$$

Thus, for the case of linear softening (Fig. 1) the value of f_{ti}^{+} can be easily defined as:

$$f_{ti}^{+} = \epsilon_u^{+} E_i \frac{D}{E_i + D} \tag{6}$$

where,

$$\epsilon_u^{+} = \epsilon_u + p\frac{f_t}{D} \tag{7}$$

The number N of teeth is automatically evaluated, depending on the arbitrary parameter p defined by the user. For smaller values of p, a higher number N of teeth is needed to cover the softening branch, leading to more exact results. In the overall procedure, the difference between the sum of *positive* triangles above the real curve and the sum of *negative* triangles below it must vanish, as shown in Fig. 1.

3 REPRESENTATION OF UNCERTAIN MATERIAL PROPERTIES

3.1 Non-Gaussian translation fields

Both Gaussian and non-Gaussian stochastic fields are used in this paper for the representation of uncertain material properties. However, the Gaussian assumption for variables bounded by physical constraints (e.g. material properties that should be strictly positive) is questionable because it leads to a non-zero probability of violation of these constraints. This is why the simulation of non-Gaussian stochastic processes and fields has received considerable attention in the field of computational stochastic mechanics.

Since all the joint multi-dimensional density functions are needed to fully characterize a non-Gaussian stochastic field, a number of studies have been focused on producing a more realistic (approximate) definition of a non-Gaussian sample function from a simple transformation of some underlying Gaussian field with known second-order statistics. Thus, if $g(\boldsymbol{x})$ is a homogeneous zero-mean Gaussian field with unit variance and spectral density function (SDF) $S_{gg}(\boldsymbol{\kappa})$ (or equivalently autocorrelation function $R_{gg}(\xi)$), a homogeneous non-Gaussian stochastic field $f(\boldsymbol{x})$ with power spectrum $S^T_{ff}(\boldsymbol{\kappa})$ can be defined as:

$$f(\boldsymbol{x}) = F^{-1} \cdot \Phi[g(\boldsymbol{x})] \tag{8}$$

where Φ is the standard Gaussian cumulative distribution function and F is the non-Gaussian marginal cumulative distribution function of $f(\boldsymbol{x})$. The transform $F^{-1} \cdot \Phi$ is a memory-less translation since the value of $f(\boldsymbol{x})$ at an arbitrary point $\boldsymbol{x}$ depends on the value of $g(\boldsymbol{x})$ at the same point only and the resulting non-Gaussian field is called a translation field [4]. Translation fields can be used to represent various non-Gaussian phenomena and have a number of useful properties such as the analytical calculation of crossing rates and extreme value distributions.

3.2 The spectral representation method

In the present work, Eq. 8 is used for the generation of non-Gaussian translation sample functions representing the uncertain material properties of the problem. Sample functions of the underlying homogeneous Gaussian field $g(\boldsymbol{x})$ are generated using the spectral representation method. This method is well suited in the context of Monte Carlo simulation (MCS) technique used for calculating the response variability of stochastic structural systems (e.g. [14]). For a two-dimensional stochastic field, the i-th sample function is given by [13]:

$$\begin{aligned} g^{(i)}(x,y) = \sqrt{2} \sum_{n_1=0}^{N_1-1} \sum_{n_2=0}^{N_2-1} [A^{(1)}_{n_1 n_2} cos(\kappa_{1n_1} x + \kappa_{2n_2} y + \phi^{(1)(i)}_{n_1 n_2} + \\ + A^{(2)}_{n_1 n_2} cos(\kappa_{1n_1} x + \kappa_{2n_2} y + \phi^{(2)(i)}_{n_1 n_2}] \end{aligned} \tag{9}$$

where $\phi^{(j)(i)}_{n_1 n_2}$, $j = 1, 2$ represent the realization for the i-th simulation of the independent random phase angles uniformly distributed in the range $[0, 2\pi]$. $A^{(1)}_{n_1 n_2}$, $A^{(2)}_{n_1 n_2}$ have the following expressions

$$A^{(1)}_{n_1 n_2} = \sqrt{2 S_{gg}(\kappa_{1n_1}, \kappa_{2n_2}) \Delta\kappa_1 \Delta\kappa_2} \tag{10a}$$

$$A^{(2)}_{n_1 n_2} = \sqrt{2 S_{gg}(\kappa_{1n_1}, -\kappa_{2n_2}) \Delta\kappa_1 \Delta\kappa_2} \tag{10b}$$

where

$$\kappa_{1n_1} = n_1 \Delta\kappa_1 \qquad \kappa_{2n_2} = n_2 \Delta\kappa_2 \tag{11}$$

$$\Delta\kappa_1 = \frac{\kappa_{1u}}{N_1} \qquad \Delta\kappa_2 = \frac{\kappa_{2u}}{N_2} \tag{12}$$

$$n_1 = 0, 1, ..., N_1 - 1 \quad and \quad n_2 = 0, 1, ..., N_2 - 1 \tag{13}$$

$N_j, j = 1, 2$, represent the number of intervals in which the wave number axes are subdivided and $\kappa_{ju}, j = 1, 2$, are the upper cut-off wave numbers which define the active region of the power spectrum $S_{gg}(\kappa_1, \kappa_2)$ of the stochastic field. The last means that S_{gg} is assumed to be zero outside the region defined by

$$-\kappa_{1u} \leq \kappa_1 \leq \kappa_{1u} \quad and \quad -\kappa_{2u} \leq \kappa_2 \leq \kappa_{2u} \tag{14}$$

The SDF used in the numerical example (see Section 5) is of square exponential type:

$$S_{gg}(\kappa_1, \kappa_2) = \sigma_g^2 \frac{b_1 b_2}{4\pi} exp\Big[-\frac{1}{4}(b_1^2\kappa_1^2 + b_2^2\kappa_2^2)\Big] \tag{15}$$

where σ_g denotes the standard deviation of the stochastic field and b_1,b_2 denote the parameters that influence the shape of the spectrum, which are proportional to the correlation lengths of the stochastic field along the x, y axes, respectively. The SDF of the translation field will be different from S_{gg} due to the spectral distortion caused by the transform of Eq. 8.

4 STOCHASTIC FINITE ELEMENT ANALYSIS

4.1 Stochastic stiffness matrix

It is assumed that the Young's modulus E, tensile strength f_t and fracture energy G_f of the material are represented by two dimensional uni-variate (2D-1V) homogeneous stochastic fields. The variation of E is described as follows:

$$E(x, y) = E_0[1 + f(x, y)] \tag{16}$$

where E_0 is the mean value of the elastic modulus and $f(x, y)$ is a zero-mean homogeneous stochastic field. The two other properties are varying in a similar way. The stochastic stiffness matrix is derived using the midpoint method i.e. one integration point at the centroid of each finite element is used for the computation of the stiffness matrix. This approach gives accurate results for relatively fine meshes as that used in the numerical example keeping the computational cost at reasonable levels [15].

Using the procedure described in the previous section, a large number N_{SAMP} of sample functions are produced, leading to the generation of a set of stochastic stiffness matrices. The associated structural problem is solved N_{SAMP} times and the response variability can finally be calculated by obtaining the response statistics of the N_{SAMP} simulations.

4.2 Variability response function approach

The concept of variability response function (VRF) has been introduced in [12] as an alternative way to MCS for computing the response variability of stochastic systems. The VRF has been established for a variety of structural systems including trusses, frames, plane stress/plane strain systems and plates with a single or with multiple correlated random properties. It is possible to express the vector of displacement variances as a function of the VRF of the system:

$$Var(\boldsymbol{u}) = \int_{-\infty}^{\infty} \mathbf{VRF}(\boldsymbol{\kappa}) S_{ff}(\boldsymbol{\kappa}) d\boldsymbol{\kappa} \tag{17}$$

A closed-form expression of $\mathbf{VRF}(\boldsymbol{\kappa})$ for plane stress/strain systems can be found in [17] where it is shown that it is a function of the deterministic parameters describing the geometry, material properties and loading of the structure. VRFs are useful mainly for two reasons: (i) they provide insight into the mechanisms controlling the response of stochastic systems and, (ii) they allow the establishment of spectral-distribution-free upper bounds on the response variability:

$$\int_{-\infty}^{\infty} \mathbf{VRF}(\boldsymbol{\kappa}) S_{ff}(\boldsymbol{\kappa}) d\boldsymbol{\kappa} \leq \mathbf{VRF}(\hat{\boldsymbol{\kappa}}) \int_{-\infty}^{\infty} S_{ff}(\boldsymbol{\kappa}) d\boldsymbol{\kappa} = \mathbf{VRF}(\hat{\boldsymbol{\kappa}}) \sigma_f^2 \tag{18}$$

where $\hat{\boldsymbol{\kappa}}$ is the wave number at which the VRF takes its maximum value. This upper bound is physically realizable and corresponds to the case in which the random field $f(x, y)$ becomes a sinusoid with random phase angle:

$$f(x, y) = \sqrt{2}\sigma_f cos(\hat{\kappa}_1 x + \hat{\kappa}_2 y + \phi) \tag{19}$$

where ϕ is a random phase angle uniformly distributed between 0 and 2π and σ_f is the standard deviation of the random sinusoid.

In addition to providing a means for computing spectral-distribution-free upper bounds on the response variability, the VRF can qualitatively reveal which types of spectral density function will cause significant response variances (see Eq. 17). That is, VRFs provide insight into the importance of the shape of the spectral density functions of the random properties on the response variance.

A VRF can be alternatively estimated numerically using a fast MCS procedure based on Eq. 17. The numerical estimation of the VRF through fast MCS is very important as the closed-form analytic expressions existing in the literature involve modulating functions that are very difficult to establish even in the simplest cases of statically indeterminate linear beams [8] or statically determinate beams with nonlinear (power) constitutive laws [16]. The fast MCS procedure can be implemented into the framework of a deterministic FE code making this approach very general. In addition, this approach is usually very efficient as convergence is achieved with a number of samples as low as 10 for each wave number.

5 NUMERICAL EXAMPLE

A symmetric notched beam [10] is analyzed in this section to illustrate the capabilities of the proposed methodology. The geometry, boundary conditions, loading and FE mesh of the beam are shown in Fig. 2. The thickness of the beam is 50 mm and the notch depth is 10 mm. Four-node linear quadrilateral elements are used with an element size of h=10mm in the vicinity of the notch and a 2x2 Gaussian integration rule in plane stress conditions. The uncertain parameters of the problem are the Young's modulus E, tensile strength f_t and fracture energy G_f of the material with mean values equal to 38 kN/mm^2, 3 N/mm^2 and 0.06 N/mm, respectively. The spatial fluctuation of the uncertain parameters is described by 2D-1V homogeneous Gaussian as well as lognormal translation stochastic fields, sample functions of which are generated using

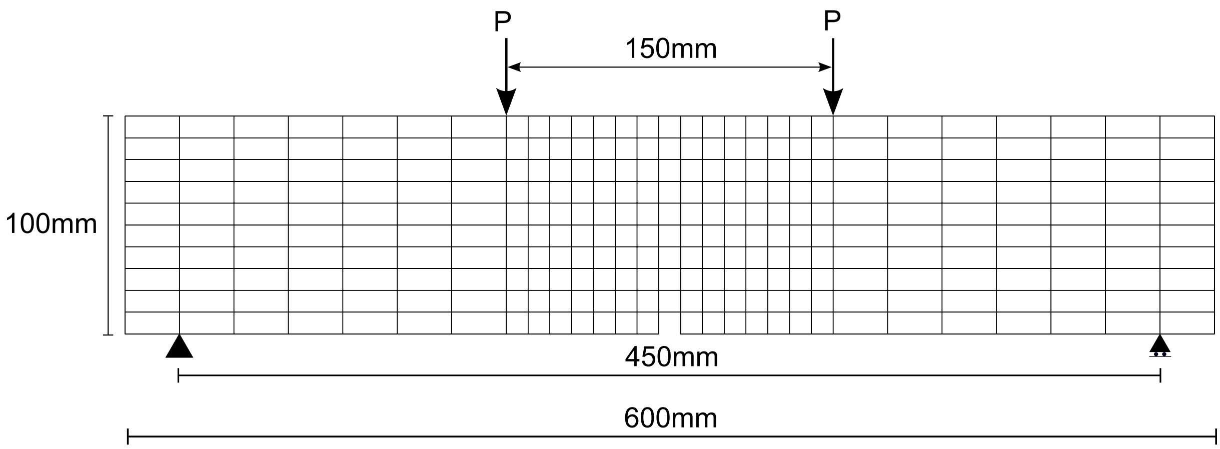

Figure 2: Notched beam (Geometry and FE mesh)

Eqs. 8, 9. Three different values ($b = 1, 10, 100$) of the correlation length parameter b ($= b_1 = b_2$) are used, corresponding to stochastic fields of low, moderate and strong correlation. The response variability is computed using MCS with a sample size equal to 100. Note that the displacement is monitored at the point where the load is applied.

Load-displacement curves corresponding to a 10% variation of E, G_f with $b = 1$ are depicted in Fig. 3. Moreover, load-displacement curves corresponding to a 20% variation of E, G_f with $b = 100$ are presented in Fig. 4. As shown in Figs. 3a, 4a, the variation of E affects the stiffness of the structure. Larger values of the coefficient of variation and of the correlation length of the stochastic fields lead to more significant variability of the load-displacement curves, as expected (Fig. 4). The response variability can also be computed using the VRF, which is shown in Fig. 5 for stochastic Young's modulus. Due to its quadrant symmetry, only a quarter of this function is shown in this figure. It is worth noting the irregular shape of the VRF, which can be attributed to the saw-tooth approach used in SLA. In addition, its computation

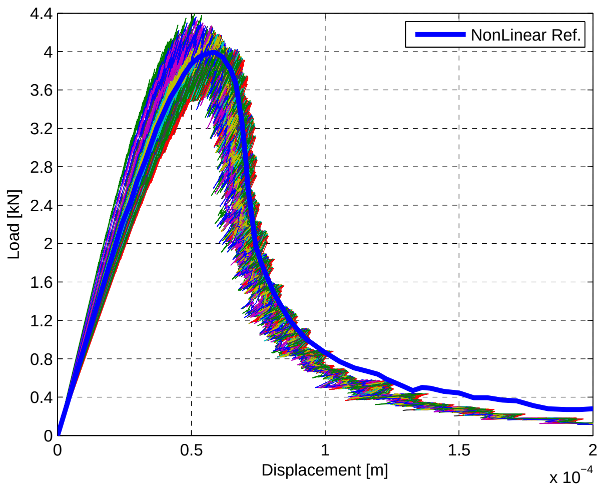

(a) Stochastic E

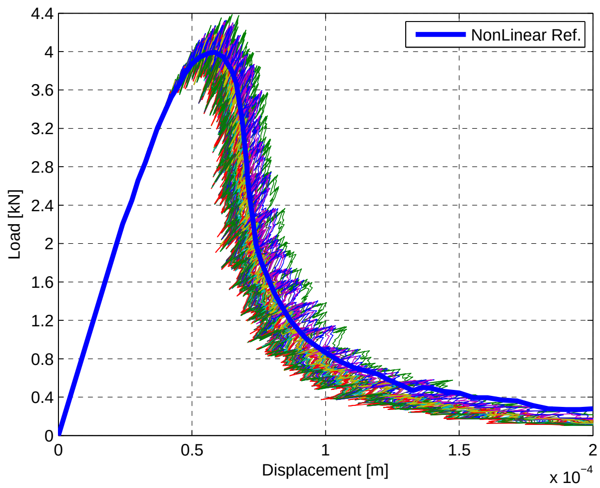

(b) Stochastic G_f

Figure 3: Load-displacement curves for stochastic parameters E and G_f with $\sigma = 10\%$ and $b = 1$ (Lognormal case).

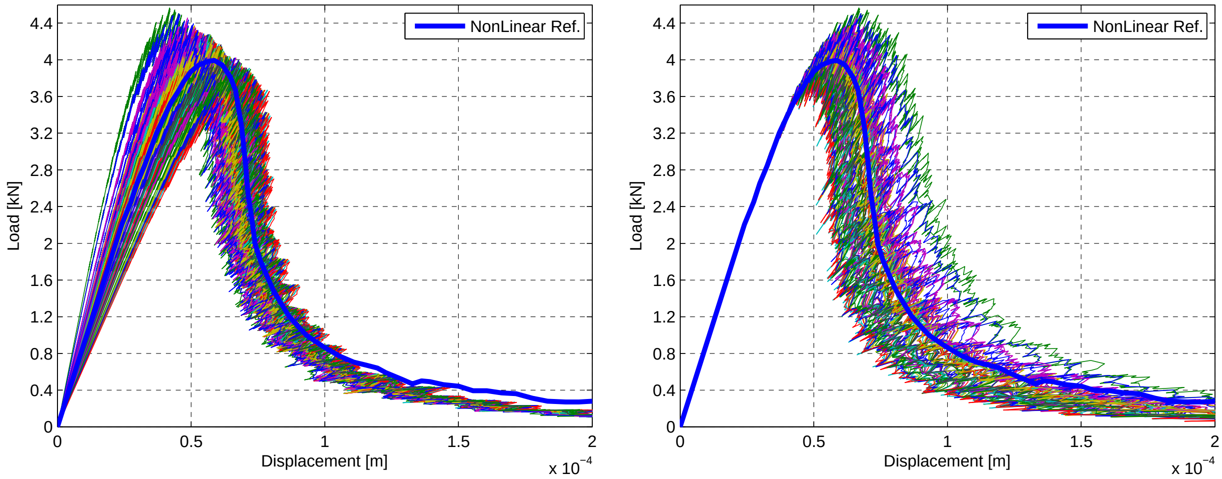

(a) Stochastic E (b) Stochastic G_f

Figure 4: Load-displacement curves for stochastic parameters E and G_f with $\sigma = 20\%$ and $b = 100$ (Lognormal case).

through fast MCS can be more expensive than direct MCS in this case (especially for a small number of samples). This is due to the fact that the whole load-displacement curve is computed for each wave number pair in the fast MCS procedure.

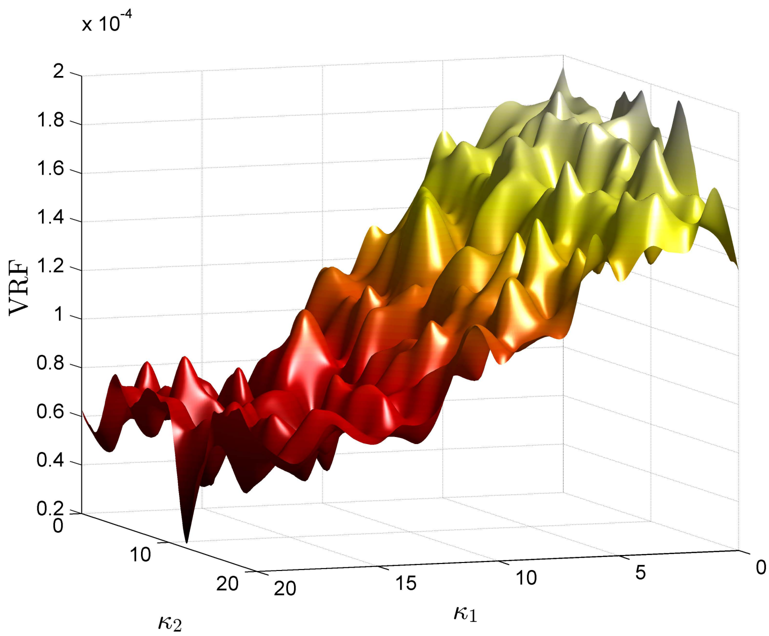

Figure 5: Variability Response Function (VRF) of peak load

6 CONCLUSIONS

In this paper, the sequentially linear analysis approach was implemented in a stochastic setting to investigate the influence of uncertain spatially varying material properties on the fracture behavior of structures made of softening materials. The uncertain properties were described by homogeneous stochastic fields using the spectral representation method in conjunction with translation field theory. The response variability was computed by means of direct Monte Carlo simulation. The influence of the variation of each random parameter as well as of the probability distribution, coefficient of variation and correlation length of the stochastic fields has been quantified. The analysis of a benchmark structure (notched beam) has shown that the load-displacement curves are affected by the spectral characteristics of the stochastic fields. The extension of SLA to the stochastic framework offers an efficient means to perform parametric investigations of the fracture behavior of structures in the case of variable material properties. The comparison of the results with existing experimental data can help to validate the assumptions made for the statistical characteristics of the stochastic fields.

ACKNOWLEDGEMENTS

This work is implemented within the framework of the research project ”MICROLINK: Linking micromechanics-based properties with the stochastic finite element method: a challenge for multiscale modeling of heterogeneous materials and structures” - Action ”Supporting Postdoctoral Researchers” of the Operational Program ”Education and Lifelong Learning” (Action’s Beneficiary: General Secretariat for Research and Technology), and is co-financed by the European Social Fund (ESF) and the Greek State. The provided financial support is gratefully acknowledged by the second author.

REFERENCES

[1] Z.P. Bažant & L. Cedolin, *Stability of Structures: Elastic, Inelastic, Fracture and Damage Theories*. World Scientific Publishing Company, 2010.

[2] M. DeJong, M. A.N. Hendriks & J.G. Rots, Sequentially linear analysis of fracture under non-proportional loading. *Engineering Fracture Mechanics*, **75**, 5042–5056, 2008.

[3] M.J. DeJong, B. Belletti, M. A.N. Hendriks & J.G. Rots, Shell elements for sequentially linear analysis: Lateral failure of masonry structures. *Engineering Structures*, **31**, 1382–1392, 2009.

[4] M. Grigoriu, Simulation of Stationary Non-Gaussian Translation Processes. *Journal of Engineering Mechanics*, **124**, 121–126, 1998.

[5] N. Moes, J. Dolbow & T. Belytschko, A finite element method for crack growth without remeshing. *International Journal for Numerical Methods in Engineering*, **46**, 131–150, 1999.

[6] J. Oliver, Modelling Strong Discontinuities in Solid Mechanics via Strain Softening Constitutive Equations. Part 1: Fundamentals. *International Journal for Numerical Methods in Engineering*, **39**, 35753600, 1996.

[7] J. Oliver, A.E. Huespe & P.J. Sanchez, A comparative study on finite elements for capturing strong discontinuities: E-FEM vs X-FEM. *Computer Methods in Applied Mechanics and Engineering*, **195**, 4732–4752, 2006.

[8] V. Papadopoulos, G. Deodatis, & M. Papadrakakis, Flexibility-based upper bounds on the response variability of simple beams. *Computer Methods in Applied Mechanics and Engineering*, **194**, 1385–1404, 2005.

[9] J. Rots, Sequentially linear continuum model for concrete fracture. *Fracture Mechanics of Concrete Structures*, in de Borst R., Mazars, J., Pijaudier-Cabot, G. & van Mier, J. (Eds.). Lisse: Balkema, 831–839, 2001.

[10] Jan G. Rots, S. Invernizzi, Regularized sequential linear saw-tooth softening model. *Int. J. Numer. Anal. Meth. Geomech.*, **28**, 821–856, 2004.

[11] Jan G. Rots, B. Belletti & S. Invernizzi, Robust modeling of RC structures with an event-by-event strategy. *Engineering Fracture Mechanics*, **75**, 590–614, 2008.

[12] M. Shinozuka, Structural Response Variability, *Journal of Engineering Mechanics*, **113**, 825–842, 1987.

[13] M. Shinozuka & G. Deodatis, Simulation of multi-dimensional Gaussian stochastic fields by spectral representation, *Applied Mechanics Reviews (ASME)*, **49**, 29–53, 1996.

[14] G. Stefanou & M. Papadrakakis, Stochastic finite element analysis of shells with combined random material and geometric properties. *Computer Methods in Applied Mechanics and Engineering*, **193**, 139–160, 2004.

[15] G. Stefanou, The stochastic finite element method: Past, present and future. *Computer Methods in Applied Mechanics and Engineering*, **198**, 1031–1051, 2009.

[16] K. Teferra & G. Deodatis, Variability response functions for beams with nonlinear constitutive laws. *Probabilistic Engineering Mechanics*, **29**, 139–148, 2012.

[17] F.J. Wall & G. Deodatis, Variability Response Functions of Stochastic Plane Stress/Strain Problems. *Journal of Engineering Mechanics*, **120**, 1963–1982, 1994.